Energy Syst (2016) 7:529–547
DOI 10.1007/s12667-015-0179-z

ORIGINAL PAPER

Dynamic modeling and power management for stand-alone AC-coupled photovoltaic system

Abouelmaaty M. Aly[1,2]

Received: 4 April 2015 / Accepted: 9 November 2015 / Published online: 26 November 2015

Abstract There are many remote areas in the world where people are living without electricity and expanding the public grids to them are uneconomical. For this reason, this paper studies a dynamic behavior of the power flow in a stand-alone AC-coupled photovoltaic (PV) system to optimize the size of the system components based on the weather conditions of the selected site and the load power demands. This system consists of a PV generator, a battery storage system (BSS), a PV inverter, a battery inverter/charger, and an AC load power. The PV generator is intermittent source of energy, so this system has to be combined with a BSS to organize the energy between the PV generator and the load. The power management uses the fuzzy power management controller to optimize the system performance by distributing the power inside the system and by managing the charge and discharge of power flow for the BSS. Real-time meteorological data of the site under study and practical load profile of a small household are used as inputs for the proposed management system. The results of the proposed system showed a good performance under various operating conditions, and maintained the state of charge of BSS at a reasonable level. In addition, the results gave a clear visualization of the behavior of the switched-mode power supply to regulate the power flow between the sources and the load on one side and to match between all components of the system on the other side. The main contributions of this work are the ability to give a mathematical model of the all components of the system and the control management which determine an optimal design of the system at any site.

✉ Abouelmaaty M. Aly
abouelmaaty67@gmail.com

1 Power Electronics and Energy Conversion Department, ERI, NRCB, Giza 12622, Egypt

2 College of Computer, Qassim University, P.O.B. 6688, Buryadah 51453, Kingdom of Saudi Arabia

Keywords Photovoltaic generator · Battery storage system · Fuzzy power management controller · Switched-mode power supply

1 Introduction

Photovoltaic (PV) systems installation have played a significant role in the world because they are pollution free, secure energy sources, and reduce the cost of electricity for remote areas [1,2]. In addition, the cost of PV generator decreases continuously, therefore these systems are economically reliable for long-term operation [3,4]. The main drawback for PV generator is the intermittent energy generation and that requires additional source of energy to improve the reliability of energy supply [5]. The battery storage system (BSS) is one of the best choices as complementary energy source in stand-alone PV systems [1–7]. In these systems, the BSS works on cyclic basis, i.e. it is charged and discharged in regular or irregular intervals during its lifetime. The management of the energy flow throughout these systems is essential to increase the life time of the BSS and to maintain a continuous energy flow [8,9].

In the literature, there are a number of studies related to control strategies for stand-alone PV systems [8–20]. These methods have used conventional approaches for controlling the power systems such as linear PI controller which has afterwards proved to be unstable in handling the various changes in weather conditions [19]. Besides these methods, there are some more advanced control techniques like the genetic algorithms, the fuzzy logic and the artificial neural networks which can readily incorporate human intelligence in complicated control systems. This paper proposes an adaptive management strategy for power flow in stand-alone AC coupled PV system based on fuzzy logic. The proposed model will optimize the active power flow between system power sources intended for different modes of operation and that it will maintain the battery state-of-charge (SOC) at a reasonable level.

There are two basic configurations to connect stand-alone PV system equipment such as PV generator and the end user [21–23]. AC and DC coupled configurations are common methods in which stand-alone systems can be configured where each with their advantages and disadvantages. AC coupled systems are more easily upgraded and expanded than a DC coupled system [21]. AC coupled accommodates multiple charging sources on the AC side of the system and does not require a charge controller to regulate DC power. AC coupled also allows direct powering of AC loads from a PV generator through PV inverter and/or a BSS through the battery inverter/charger. This integration method offers the possibility of combining multiple power sources or mixing power generation systems that would either be impossible or very inefficient to achieve in a traditional DC coupled system. In many ways, AC coupled allows to maximize the benefits that many individual systems have to offer. In this paper, stand-alone AC coupled PV system, as shown in Fig. 1, will be studied. The BSS either absorbs any surplus of energy produced by PV generator or supplies any shortage of energy to meet the AC load power [2,4].

The aim of this work is to study the stability and dynamic behavior of the AC coupled PV system, which has multiple operating modes. In this configuration the PV source and the BSS are connected to an AC bus through the switched-mode power supplies

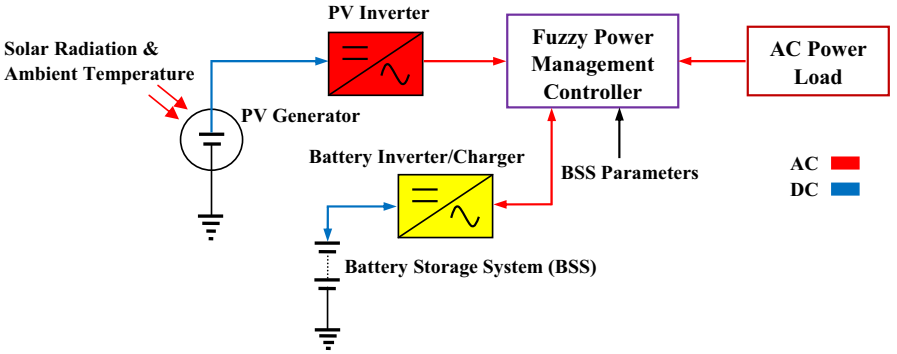

Fig. 1 Stand-alone AC-coupled PV power system

(SMPSs). As the weather conditions and the SOC of the BSS vary with time during a day, the system must be designed to operate with multiple operating modes. Thus, the system design has to take into consideration the different modes of operation. The dynamics of such a system has been rarely discussed in the literature. Also, this paper deals with the fuzzy power management controller (FPMC) to maintain the power balance and stable operation of the system under any conditions and also to optimize the size of the system components. The simulations of the system's performance are carried out with typical weekly solar radiation and ambient temperature data from one site in Egypt at two different weather conditions. The produced electricity was analyzed for this site at 1 week in winter and summer seasons.

The paper is organized as follows: Sect. 2 presents the dynamic model of the power system components. The proposed control structure and the operating modes are addressed in Sect. 3. The meteorological data and the load profile of the selected site are presented in Sect. 4. Implementation of the proposed system represents in Sect. 5. The results and their analysis are presented in Sect. 6. Finally, the conclusions are given in Sect. 7.

2 Dynamic modeling of the power system components

The proposed power system consists of a PV generator, a BSS, a PV inverter, a battery inverter/charger, and a FPMC. Modeling of the system components plays an important role in the sizing calculation [3,15]. These models are summarized in the following subsections.

2.1 Modeling of PV generator

The energy generated by a PV generator directly depends on the weather conditions (solar radiation and ambient temperature) and the installed peak power [5,16]. However, there are a number of reasons that causes a decrease in the expected energy such as ohmic losses, mismatch losses, low radiation losses, dirt and dust losses, SMPS, and so on. Thus, the energy generated by a PV generator for any period of time such as

a day, week, month, or year can be estimated to study the effect of these factors on the performance of the overall the system. It is a very complicated task to determine the exact value of each type of losses for a system [24]. Therefore, the number of losses will be neglected in this study that takes this into account at determining the size of PV generator by multiplying the exact size of PV generator in a factor around 1.5 to 2 [24]. A single diode model is used to estimate the power provided by a PV generator and it defines the current/voltage characteristic of the module as the following expression [5]:

$$I_m = [I_{SC,STC} + \epsilon(T_{sm} - T_{sm,STC})] \times \frac{S_R}{1000} - I_{RSC}\left(\frac{T_{sm}}{T_{sm,STC}}\right)^3 e^{[(\frac{E_g \times q}{A_I K})(\frac{1}{T_{sm,STC}} - \frac{1}{T_{sm}})]}\left(e^{(q\frac{V_m + I_m \times R_m}{A_I K T_a})} - 1\right) \quad (1)$$

where, I_m (A) is the module current, V_m (V) is the module voltage, $I_{SC,STC}$ (A) is the short circuit current of the module at Standard Test Condition (STC), ϵ (A/°C) is the current temperature coefficient, $T_{sm,STC}$ (°C) is the module temperature at STC, T_{sm} (°C) is the module temperature, S_R (W/m^2) is the solar radiation, I_{RSC} (A) is the reference saturation current at STC, E_g (eV) is the energy gap, q(C) is the charge of electron, A_I is the ideality factor, K (m^2 kg/s^2 K) is the Boltzmann constant, and T_a (K) is the ambient temperature. STC means that $S_R = 1000$ W/m^2, $T_a = 25$ °C, and air mass $AM = 1.5$. The series resistance of the module $R_m(\Omega)$ is [25]:

$$R_m = \frac{P_{MPP,STC}}{I^2_{MPP,STC}} - \frac{V_{OC,STC}}{20.7}\left(\frac{1}{I_{SC,STC} - I_{MPP,STC}}\right) \quad (2)$$

where, $P_{MPP,STC}$ (W) is the output power of the module at maximum power point (MPP), $I_{MPP,STC}$ (A) is the module current, $V_{OC,STC}$ (V) is the module open circuit voltage, and $I_{SC,STC}$ (A) is the module short circuit current at STC. The Newton's method is used to obtain the value of the module current at any value of the module voltage. There are many different algorithms to reach the maximum output power of the module for a given pair of values S_R and T_a. The output power of the PV generator at MPP equals $P_{MPP} \times N_P \times N_S$. Here, N_P is the number of modules connected parallel and N_S is the number of modules connected series. Figure 2 illustrates the match between the mathematical model for one module (Polycrystalline SW140 R6A) and the experimental results under three different operating conditions.

2.2 Modeling of nickel metal hydride battery

Nickel Metal Hydride (NiMH) battery has begun to find its use in stand-alone PV systems [26,27]. The energy density of this type is more than double compared to lead acid and 40 % higher than that of nickel cadmium (NiCd) battery [28]. In addition, it accepts both higher charge and discharge rates. Like NiCd battery, NiMH battery is susceptible to a "memory effect", although to a lesser extent. It is more expensive than lead–acid and NiCd batteries, but it is considered better for the environment.

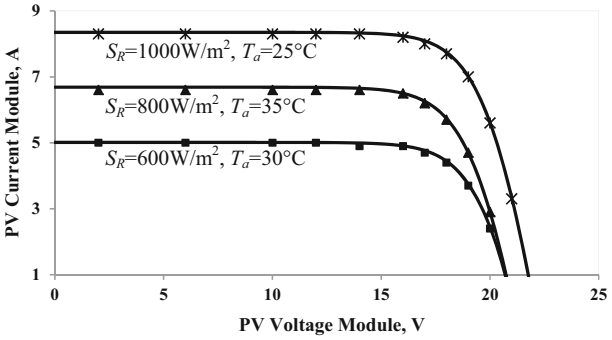

Fig. 2 I–V model curves versus experimental points for one PV polycrystalline module SW140 R6A

The operating temperature range for NiMH cells has been extended to over 100 °C (−30 to +75 °C), which far exceeds the temperature range currently achievable by lithium cells making NiMH technology ideal for any weather conditions [26]. Some advantages of NiMH battery are: high energy density (50 % better than NiCd and 60 % better than lithium ion), lifetime is 3000 cycles at 100 % Depth of Discharge (DOD) but the lifetime can be expected more than 350,000 cycles at lower DOD (for example at 4 % DOD), flat discharge characteristic, wide operating temperature range, rapid charge possible in one hour, environmentally friendly (no cadmium or lead), and much safer than lithium based cells in case of abuse due to the use of more benign active chemicals [26]. Disadvantages of this type of battery are: high rate discharge is not as good as NiCd, less tolerant of overcharging than NiCd, high self discharge rate, lower capacity, the cell voltage is only 1.18 V which means that many cells are required to make up high voltage battery, and the cost is high which is around three times compared to lead acid battery for large capacity. The mathematical model of NiMH battery represented in charge and discharge modes can be shown as follows [9]:

For charging mode ($i_b < 0$)

$$U_b = U_0 - R_b i_b - P\frac{Q \times i_b^*}{C_E + 0.1Q} - P\frac{Q \times C_E}{Q - C_E} + A \times e^{-B\int i_b dt} \tag{3}$$

For discharge mode ($i_b > 0$)

$$U_b = U_0 - R_b i_b - P\frac{Q \times (C_E + i_b^*)}{Q - C_E} + A \times e^{-B\int i_b dt} \tag{4}$$

where, U_b (V) is the nonlinear battery voltage, U_0 (V) is the battery constant voltage, R_b (Ω) is an internal battery resistance, P (Ah^{-1} or Ω) is the polarization constant or polarization resistance, C_E (Ah) is the extracted capacity, Q (Ah) is the battery capacity, A (V) is the exponential voltage, and B (Ah^{-1}) is the exponential capacity. Both the battery current i_b (A) and filtered current i_b^* (A) will be positive if the battery is in discharge mode and vice versa. The SOC is calculated as [3]:

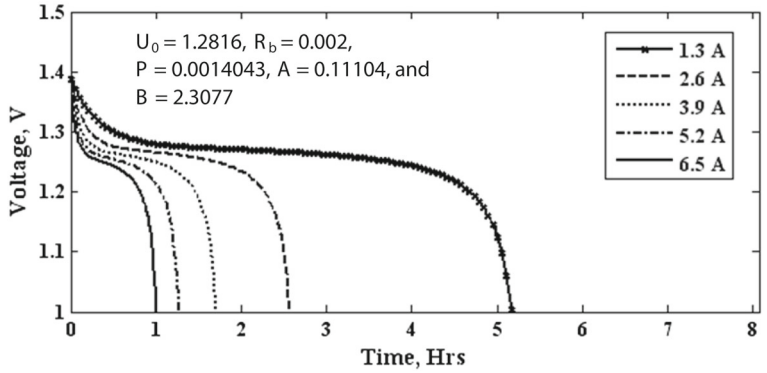

Fig. 3 A discharge behavior for one cell of NiMH battery at different values of discharge current as the nominal discharge current is 1.3 A

$$SOC\ (\%) = 100\left(1 - \frac{1}{Q}\int_0^t i_b dt\right) \tag{5}$$

A typical discharge behavior for one cell of NiMH battery at different values of discharge currents is shown in Fig. 3. It is clear that the discharge time drastically decreases with the increase in discharge current. With the nominal current of 1.3 A, the cell battery can provide power for a little more than five hours. However, at a large current 6.5 A, it can provide power only for around one hour before it is fully discharged. The battery capacity Q (Ah) was calculated using the following relation [2]:

$$Q = \frac{N_{cd} E_L}{DOD \times \eta_b} \tag{6}$$

where, N_{cd} is the largest number of continuous cloudy days of the site under a study area, E_L is the average energy load consumed, DOD = SOC − 1 is the maximum permissible depth of battery discharge, and η_b is the battery efficiency.

2.3 Modeling of switched-mode power supply

The SMPSs are very important in the proposed system to increase the efficiency of PV generator by operating at MPP and maintain the lifecycle of the battery by organizing the charge and discharge operations [21]. The SMPSs are also used to match between the voltages of the system components which are generated by PV generator and the BSS on one side and the required AC power load demand on the other side. The output power (P_o) of the SMPS is related to input power (P_I) by [29,30]:

$$P_O = \alpha + \beta P_I + \gamma P_I^2 \quad \text{when } P_{off} \le P_I \le P_{Max} \tag{7}$$

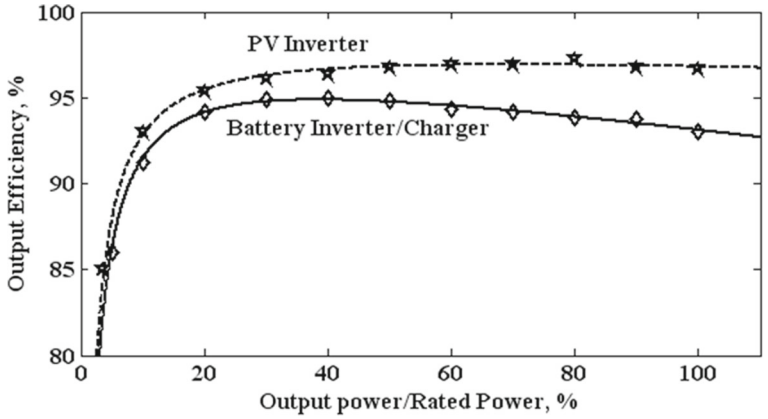

Fig. 4 Output efficiency model curves versus experimental points for PV inverter (Sunny Boy 3000TL) and battery inverter/charger (Sunny Island 3.0M)

where P_{off} (W) is the standby power, P_{Max} (W) is the maximum output power, and α, β, and γ are the fitting parameters. These parameters represent the self power consumption, the voltage drop, and the ohmic losses of the SMPS respectively.

The system under study has two SMPSs. PV inverter has two control modes which are maximum power point tracking (MPPT) control and constant voltage control (CV) [31]. It converts directly the DC power from the PV generator to supply the AC power load demand. Battery inverter/charger is the central component in the proposed system and it performs a multiple important tasks for a system to maintain the BSS [21,22]. It converts the DC electricity stored in batteries to regular AC power load demand when the PV generator is either insufficient or unavailable. When the PV generator is available and more than the AC power load demand, the inverter/charger will recharge the BSS for later use. Figure 4 illustrates the match between the mathematical model and the experimental results for PV inverter and battery inverter/charger output efficiencies.

3 Fuzzy power management controller and operation modes

To operate the designed system safely and stable, the FPMC should manage the power flow between the system sources, the PV generator (P_G), BSS (P_B), and the AC load power (P_L). The dynamic constraints of the BSS should also be considered [32]. The main relation between these units is:

$$P_L - P_G = P_B \tag{8}$$

As shown in Table 1 and Fig. 5, there are six possible operating modes:

For *Mode 1*, the AC output power of the PV generator which is manipulated by using the PV inverter with MPPT can provide enough energy to AC load power. The surplus energy is used to charge the BSS (P_{Bch}) through the battery inverter/charger.

Table 1 Operating modes of the proposed PV power system

State	$P_G = 0$ (at night or cloudy weather)	$P_G \neq 0$	
		$P_G \geq P_L$	$P_G < P_L$
$SOC \leq SOC_{Lo}$	Mode 6 System off	Mode 1 $P_L = P_G$ and $P_{Bch} = P_L - P_G$	Mode 5 $P_{Bch} = -P_G$ and $P_L = 0$
$SOC_{Lo} < SOC < SOC_{Hi}$	Mode 3 $P_L = P_{Bdis}$	Mode 1 $P_L = P_G$ and $P_{Bch} = P_L - P_G$	Mode 2 $P_L = P_G + P_{Bdis}$
$SOC \geq SOC_{Hi}$	Mode 3 $P_L = P_{Bdis}$	Mode 4 $P_L = P_G$ CV mode	Mode 2 $P_L = P_G + P_{Bdis}$

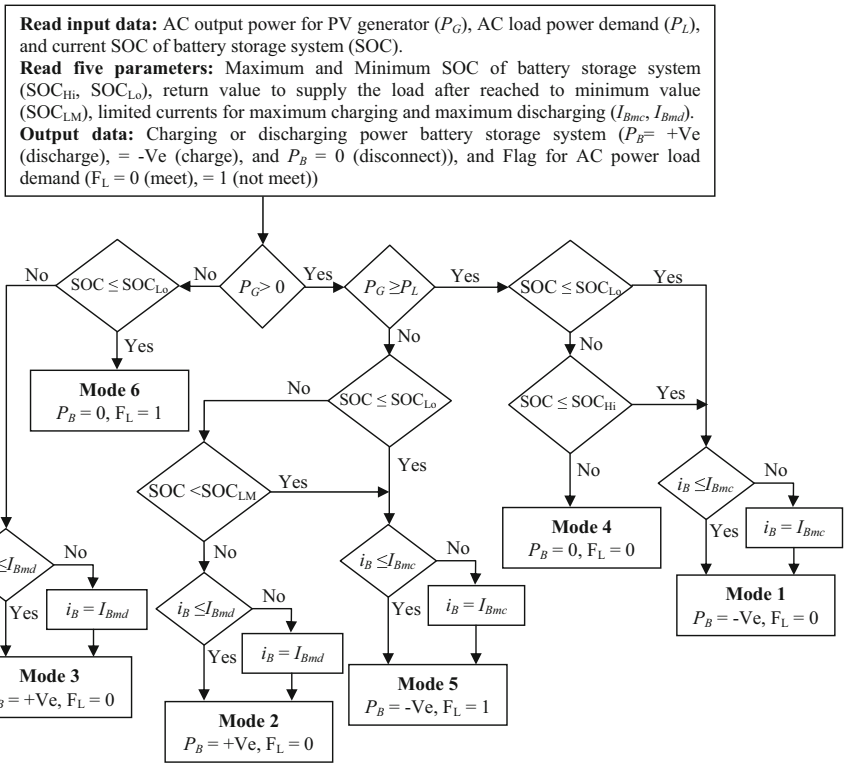

Fig. 5 A *flow chart* for proposed power management algorithm of the system

At *Mode 2*, the output power of the PV generator cannot provide enough energy to AC load power. Therefore, the shortage energy will be complemented by discharging the BSS (P_{Bdis}).

Mode 3 occurs at cloudy weather or at night, when the output power of the PV generator is zero. Then, the PV inverter stops working, and the battery inverter operates to supply power for the AC load.

For *Mode 4*, the output power of the PV generator can provide enough energy to the AC load power and the SOC is greater than or equal to the maximum limit (SOC_{Hi}). Therefore, the charger stops working and the PV inverter must immediately change to normal operating mode, i.e, CV.

At *Mode 5*, the output power of the PV generator is less than the AC load power and the SOC is less than or equal to the minimum limit (SOC_{Lo}), the system disconnects the AC load power and works only to charging the BSS.

For the last operating mode (*Mode 6*), the output power of the PV generator is zero and the SOC is less than or equal to the minimum limit. Then, the whole system stops to protect the BSS from damage.

In this system, to ensure the normal operation for Mode 3, the maximum discharging power of the BSS (SOC_{Lo}) and the power rating of the battery inverter should be higher than the critical AC load power. The PV inverter should be designed to be capable of transferring maximum PV generator to the AC load power and the surplus power is used to charge the BSS. The maximum available power of PV generator should be around two times greater than the maximum AC load power to ensure that the system operates normally at night or cloudy weather. The size of the BSS should also be at least three times greater than the AC load power to be able to compensate for the absence the PV generator at night or cloudy weather. The permanent changes in the AC load power and unpredictable load profile are unavoidable. In addition, the non-linear subsystems add to the complexity of the structure of the system [11]. Hence, a FPMC is presented to adapt the weather conditions, AC load power, and the battery SOC, as shown in Fig. 1.

The FPMC maintains the SOC at a reasonable level ($SOC_{Lo} = 40\ \%$ and $SOC_{Hi} = 95\ \%$ in this work). It also protects against current limited (I_{Bmc} and I_{Bmd}) by controlling the power level required from the battery (P_B). The FPMC relates these values by using a list of *if–then* statements called rules [8]. The *if*-condition describes the fuzzy sets of the input variables. In this work, the fuzzy variables P_G, P_L and SOC are described by fuzzy singleton. The fuzzy rules are in the form:

$$\textit{Rule } i : \textbf{IF } P_G \text{ is } X_i \text{ and } P_L \text{ is } Y_i \text{ and SOC is } Z_i, \textbf{THEN } P_B \text{ is } M_i,$$

where X_i, Y_i and Z_i are fuzzy subsets in their universes of discourse and M_i is fuzzy singleton. Each universe of discourse is divided into three fuzzy subsets (low, medium and high). The fuzzy subsets and the membership functions are evaluated to obtain the output controller by using the *then*-condition.

4 Meteorological data and load profile of the selected site

The proposed stand-alone AC coupled PV system is located in Egypt/El-Hamam with longitude 29.57°E and latitude 31.12°N. Figure 6 shows the weekly solar radiation, the ambient temperature, and the load profile which were measured every 15-min

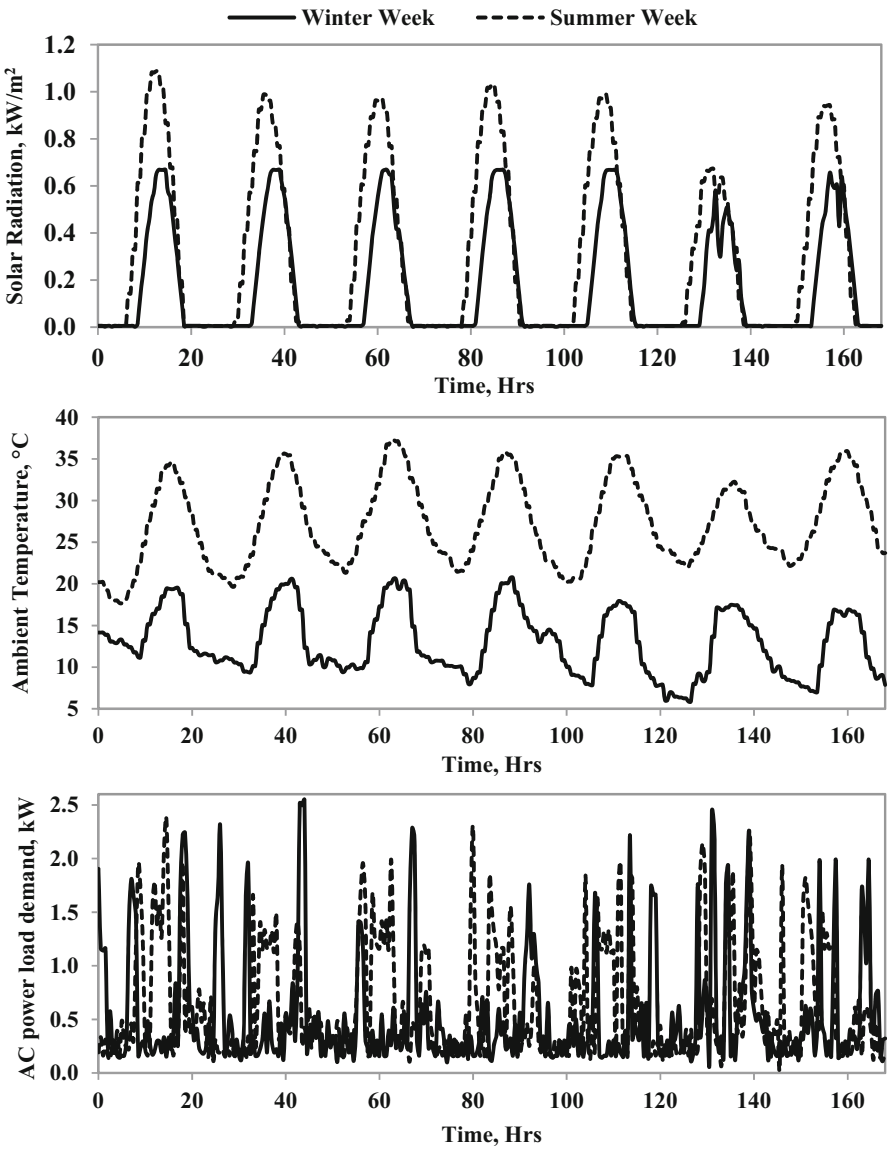

Fig. 6 The weekly solar radiation, ambient temperature, and load profile at Egypt/El-Hamam for winter and summer seasons

periods. At this site, the average weekly solar radiations for the two cases under study, 1 week for each winter and summer seasons, are 4.17 and 7.48 kWh/m^2/day respectively. The weekly average ambient temperature of this site for the two cases is 13 and 27.3 °C respectively. A practical load profile represents the average AC electric power consumption for the small household over 1 week period in winter and summer seasons for the site under study. The average energy consumption of AC electrical load power demand for winter and summer day is 13.23 and 15.35 kWh/day respectively.

5 Proposed system implementation

Based on the discussed models in the preceding sections, the proposed system can be implemented and the simulation results are obtained by developing a detailed MATLAB/SIMULINK software package.

To evaluate the dynamic performance of the proposed system, the system should be simulated at least over a year, which requires a large space of memory to store the data of the overall system. Therefore, two cases are selected from one year to test and analyze the results. The first case is considered the worst case where the weather conditions are cloudy. The components of the system will be adjusted based on this case and the system is simulated over 1 week. Second case, the system is simulated without any changes in the values of parameters, only the solar radiation and the AC power load will be changed based on the system simulation period, which is 1 week in the summer season.

From the load profile shown in Fig. 6, the hourly load consumption considered maximum as the load requirement. Thus, the PV generator for the proposed system should produce energy that equals approximately 2 times the energy consumption. In this site, the average sunlight in winter and summer days is 9 and 12 h respectively. Therefore, the size of PV generator to produce 26.46 kWh/day for winter week (worst case) is 2.94 kW. As the proposed system is intended to supply 13.23 kWh/day, the largest number of continuous cloudy days in the selected site is considered 3 days, and the DOD and the battery efficiency are limited by 60 and 90 % respectively. Then the battery capacity according to the Eq. (6) becomes 72.5 kWh. In this work, the voltage in the DC side is selected as 48 V. Thus, the battery capacity is approximately 1500 Ah. Figure 7 shows the BSS capacities versus the AC load power demand for the worst case study.

The technical specifications of the main components and their parameters' values which are used to model and simulate the proposed system depicted in Fig. 1 are given in Table 2.

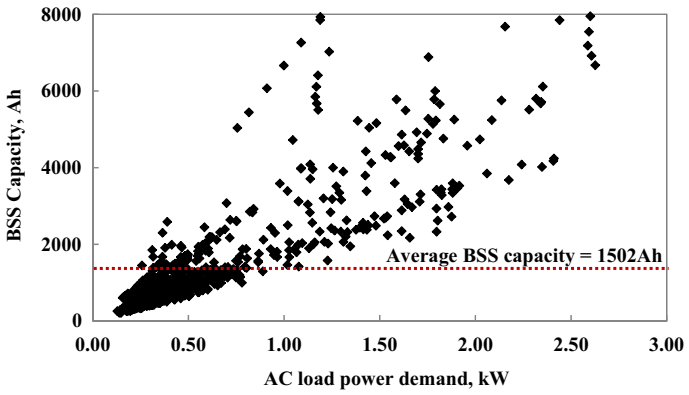

Fig. 7 The BSS capacities versus the AC load power demand for the worst case study (weekly winter)

Table 2 Technical specifications of the modeled components of the proposed PV system

Components	Parameters
PV generator	Type: Polycrystalline SW140 R6A,
	Module: 36 cells
	STC: $S_R = 1000$ W/m^2, $T_a = 25$ °C, $AM = 1.5$
	NOCT: 46 °C
	Model parameters: $I_{SC,STC} = 8.35$ A, $V_{OC,STC} = 22.1$ V, $I_{MPP,STC} = 7.85$ A, $V_{MPP,STC} = 18$ V, $P_{MPP,STC} = 140$ W, current temp. coefficient = 0.081 %/K, voltage temp. coefficient = −0.37 %/K, P_{MPP} temp. coefficient = −0.45 %/K, cell area = 243.36 cm^2, series modules $N_s = 21$, and parallel modules $N_P = 1$
BSS	Type: NiMH
	Model parameters: series cells $N_{sb} = 41$, parallel cells $N_{pb} = 231$, nominal voltage $(1.18 \times N_{sb}) = 48$ V, rated capacity $(6.5 \times N_{pb}) = 1500$ Ah, maximum capacity $(7 \times N_{pb}) = 1617$ Ah, fully charged voltage $(1.39 \times N_{sb}) = 55.6$ V, nominal discharged current $(1.3 \times N_{pb}) = 300$ A, internal resistance $(0.002 \times N_{sb}/N_{pb}) = 0.000346\Omega$, capacity at nominal voltage $(6.25 \times N_{pb}) = 1443.75$ Ah, exponential zone voltage $(1.28 \times N_{sb}) = 51.2$ V, and exponential zone capacity $(1.3 \times N_{pb}) = 300$ Ah
SMPS	PV inverter (Sunny Boy 3000TL)
	Model parameters: maximum power input $(P_{max,in}) = 3200$ W, input voltage range at MPP $(V_{MPP}) = 175-500$ V, maximum input current $(I_{max,in}) = 15$ A, rated output power $(P_{rated,S}) = 3000$ W, nominal AC output voltage $(V_{ac}) = 220-230$ V, and maximum output current $(I_{max,out}) = 16$ A. The fitting parameters are: self power consumption $(\alpha) = -18.40$ W, the voltage drop $(\beta) = 0.986$, and the ohmic losses $(\gamma) = -3.98 \times 10^{-6}$ W^{-1}
	Battery inverter/charger (Sunny Island 3.0M)
	Model parameters: AC voltage rated $(V_{rated}) = 230$ V, AC rated current $(I_{rated}) = 10-60$ A, AC rated power $(P_{rated,B}) = 2300$ W, DC side: rated voltage $(V_{rated,dc}) = 48$ V, voltage range $(V_{DC}) = 41-63$ V, maximum charging current $(I_{max,C}) = 51$ A, rated charging current $(I_{rated,C}) = 45$ A, and DC discharging current $(I_{max,D}) = 51$ A. The fitting parameters are: self power consumption $(\alpha) = -16.02$ W, the voltage drop $(\beta) = 0.983$, and the ohmic losses $(\gamma) = -18.44 \times 10^{-6}$ W^{-1}

6 Discussion of the results

The aim of this work is to study and compare the dynamic performance of the proposed system under two different weather conditions for the same site, as shown in Fig. 6. Before analyzing the simulation results of the system, a quick look at the behavior of the solar radiation and the AC load power should be considered.

The energy and relative time distributions for the two cases are shown in Figs. 8 and 9. From these figures, it is clear that the energy distribution of S_R has similar behavior for the two cases of study, but is limited by 750 W/m^2 for weekly winter season and by 1100 W/m^2 for weekly summer season. The relative time distribution of S_R is also approximately similar for the two cases, but is confined in narrower range (100–750 W/m^2) for winter season than summer season (100–1100 W/m^2). As for

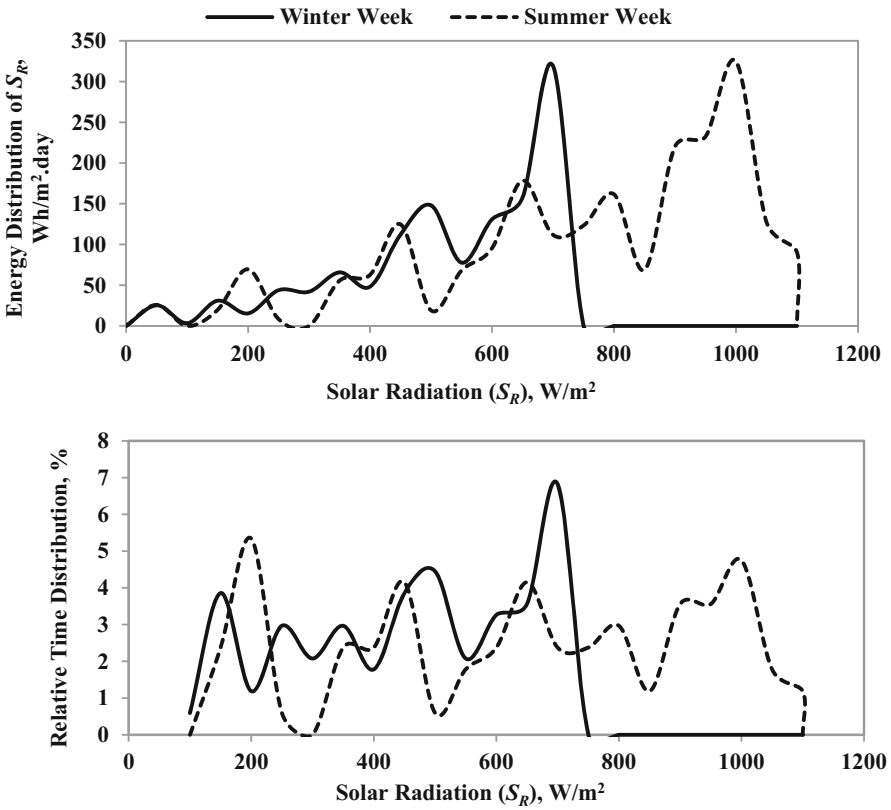

Fig. 8 Energy and relative time distributions for weekly solar radiation of two cases studies

the AC load power, the energy distribution is similar for the two cases; the AC load power is less than or equal to 1 kW, but at higher than this value some differences occur. The relative time distribution of the AC load power illustrates that the required power always occurs at low power less than 0.5 kW for the two cases. These curves are important for optimizing the design of the SMPS coupled with the PV generator and the BSS which will be discussed in this section later.

The DC output power of PV generator related to the DC output voltage at MPP and the output AC power of PV generator related to time for the two cases are shown in Fig. 10. The behaviors of the DC output power for two cases are similar but for the winter season the average values of the power moves to the high values of the output voltage or moves to low values of the output voltage for summer season. This means that, the DC output power at MPP for winter season or cloudy weather is close to open-circuit voltage of the PV generator; while for clear weather or summer season it close to short-circuit current of the PV generator. The average efficiency of the PV generator for the two cases is 10.21 and 13.84 % in winter and summer seasons respectively. From the AC output power of the PV generator, it is clear that the average sunlight over the day and the power produced in summer season is larger than in winter

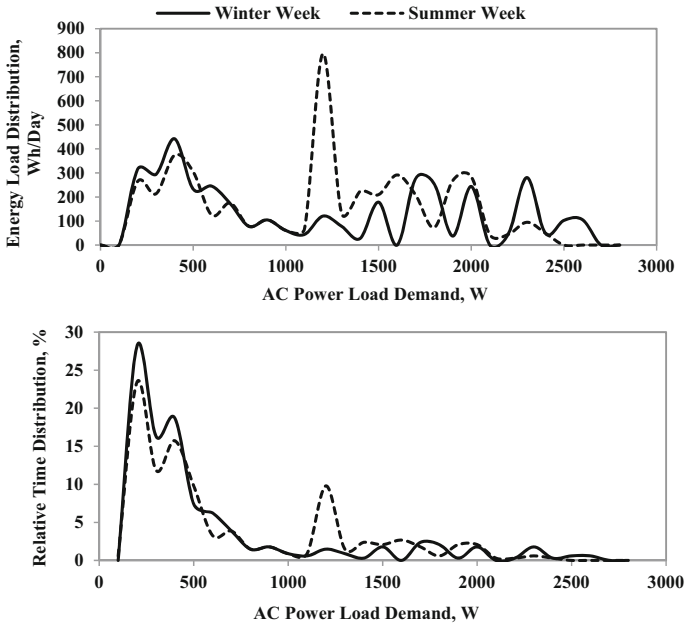

Fig. 9 Energy and relative time distributions for weekly AC power load demand of two cases studies

season and also these curves are more influenced by the solar radiation, see Fig. 6. Charging/discharging power and SOC of the BSS are shown in Fig. 11. The battery inverter/charger is employed to regulate the discharging and charging operations. If the battery has not been fully charged, that means its SOC is less than 95 %, the battery will be charged in Modes 1 and 5. Also, if the battery has not been fully discharged, that means its SOC is greater than 40 %, the battery will be discharged in Modes 2 and 3.

The charging/discharging of a BSS is determined by the output power coming from FPMC, P_B, to the BSS. When P_B is positive ($P_G < P_L$), the battery inverter is used for discharging the BSS and it protects the BSS by monitoring the discharge current which it cannot increase more than the maximum discharge current (I_{BMD}). When P_B is negative ($P_G > P_L$), the battery charger is used for charging the BSS and it protects the BSS by monitoring the charge current which it cannot increase more than maximum charge current (I_{BMC}). The over-charging protection and over-discharging protection have been taken into account by introducing maximum and minimum SOC (SOC_{Hi} and SOC_{Lo}).

Also, from Fig. 11, it is clear that the SOC reaches the maximum limit every day for the summer case but for the winter case this phenomenon is not achieved. The reason for this is the average energy supplied from the PV generator during the time day in winter case is 10.72 kWh based on the weather conditions. This value of generated energy is less than the average daily energy load for this case, i.e., 13.23 kWh. Therefore, the BSS compensates the shortage generated energy. Unlike in the summer case, as the

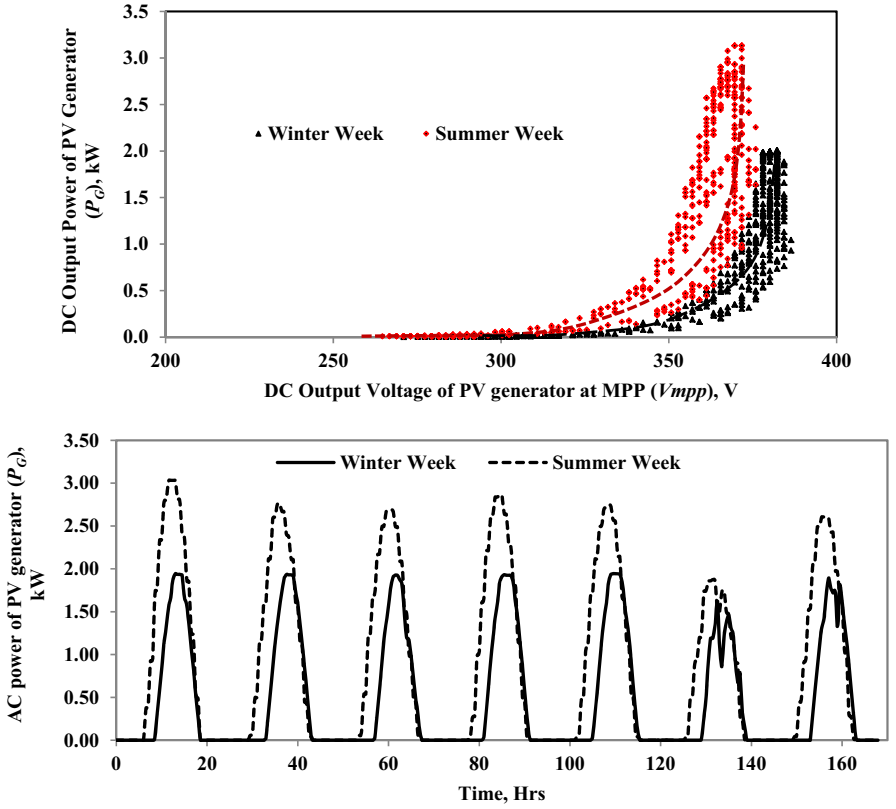

Fig. 10 DC output power versus DC output voltage at MPP and AC output power versus time for PV generator

generated energy is 16.68 kWh which it is greater than the average daily energy load for this case, i.e., 15.35 kWh.

The relative time distribution efficiencies for the SMPS of the proposed system at the two cases under study are shown in Fig. 12. From this figure, it is clear that over 90 % for the operation time of the BSS charger at the cases under study, the efficiency is ranged between 90 and 95 %. Therefore, the average battery charger efficiency is 92.61 and 92.25 % for the weekly winter and summer seasons respectively. Also, for the BSS inverter (Sunny Island), around 30 % for the operation time at the cases study the efficiency is ranged between 90 and 95 % and around 65 % for the operation time the efficiency is ranged between 95 and 100 %. To simplify this discussion, over 95 % for the operation time of the BSS inverter at the cases study, the efficiency is ranged between 90 and 100 %. Therefore, the average BSS inverter efficiency is 95.45 and 94.78 % for the weekly winter and summer seasons respectively.

By the same way for the PV inverter (Sunny Boy), around 15 % for the operation time at the cases study the efficiency is ranged between 90 and 95 % and around 75 % for the operation time the efficiency is ranged between 95 and 100 %. Thus, over 90 %

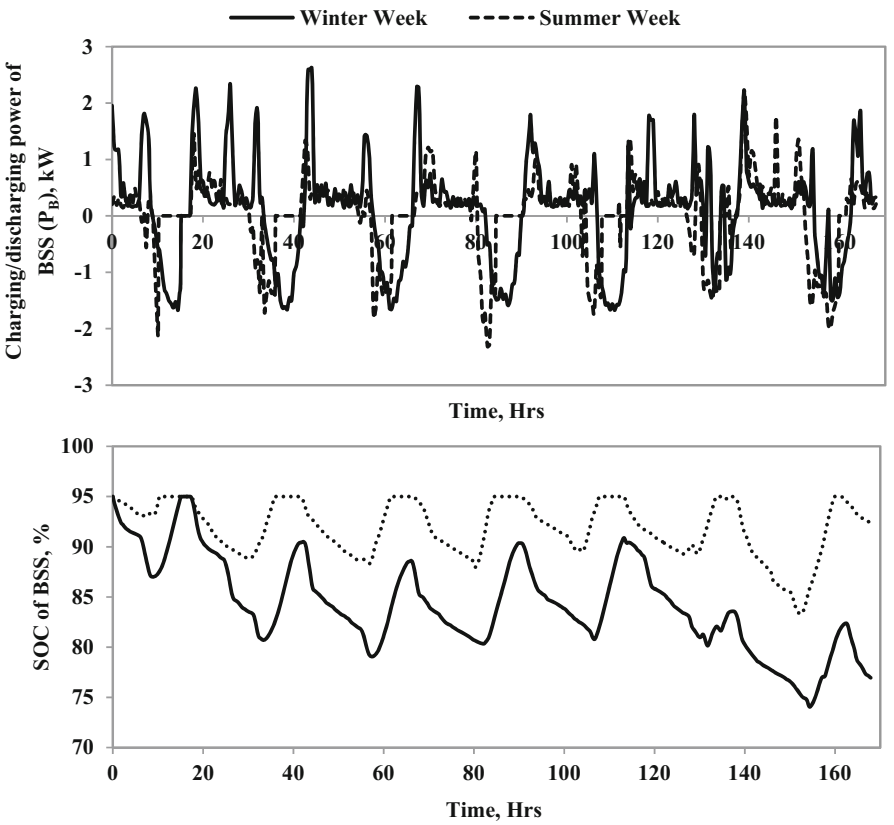

Fig. 11 Charging/discharging power and SOC of BSS at two cases study

for the operation time of the PV inverter at the cases study, the efficiency is ranged between 90 and 100 %. Therefore, the average PV inverter efficiency is 92.68 and 92.22 % for the weekly winter and summer seasons respectively. For the all SMPS, around 5 % or less for the operation time at the cases study the efficiency is ranged between 80 and 90 %.

7 Conclusions

In this paper, the dynamic behavior of a stand-alone AC coupled PV system is studied for short-time operation in Egypt/El-Hamam site. All components of the system are modeled and validated before they are used in the system. The system is simulated over two different cases at the selected site to give a real visualize about the performance of the system during the whole year. When meteorological data and the load power fluctuate, the output power of PV generator will change. Battery storage system can be charged or discharged to maintain the power balance between PV generator and the AC power load, thus improving the stability of the entire system. Fuzzy power controller

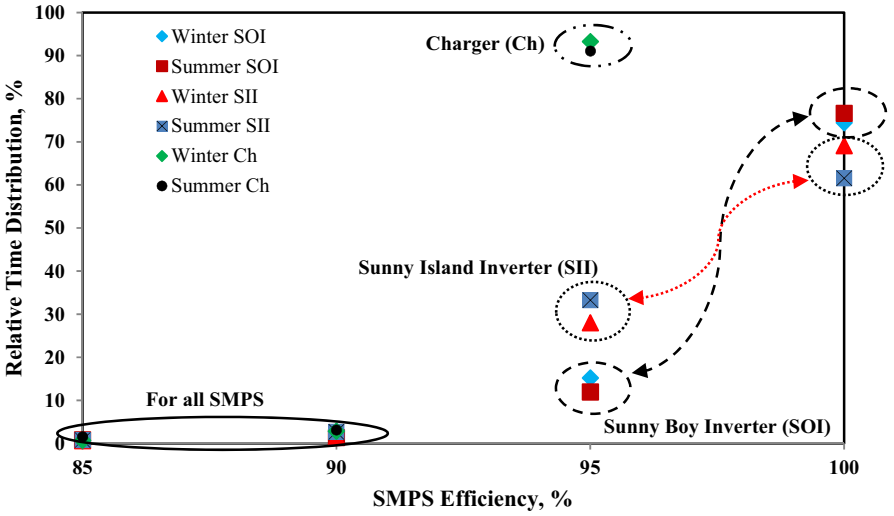

Fig. 12 Relative time distribution efficiency for SMPS of the proposed system at two cases study

optimizes the system performance and maintains the state of charge of the battery storage system at a reasonable level. The results show that the average daily load requirement of a small household for weekly winter and summer seasons is 13.23 and 15.35 kWh/day respectively. Therefore, 21 PV modules with 140 Wp rated power are used to meet these loads. The average energy supplied from the PV generator during the time day is 10.72 and 16.68 kWh. The battery storage system (48 V, 1500 Ah) during the night time is employed to meet the night power load.

References

1. Thongsawaeng, C., Audomvongseree, K.: Determination of the optimal battery capacity of a grid-connected photovoltaic system with power and frequency fluctuations consideration. In: 10th International Conference on Electrical Engineering/Electronics, Computer, Telecommunications and Information Technology (ECTI-CON), Krabi, Thailand, pp. 1–6 (2013)
2. Abdulateef, J.: Simulation of solar off-grid photovoltaic system for residential unit. Int. J. Sustain. Green Energy **4**(3–1), 29–33 (2014)
3. Delavaripour, H., Karshenas, H.R., Bakhshai, A., Jain, P.: Optimum battery size selection in standalone renewable energy systems. In: 33rd International Telecommunications Energy Conference (INTELEC), Amsterdam, Netherlands, pp. 1–7 (2011)
4. Mahmood, H., Michaelson, D., Jiang, J.: Control strategy for a standalone PV/battery hybrid system. In: 38th Annual Conference on IEEE Industrial Electronics Society, Montreal, QC, pp. 3412–3418 (2012)
5. Ding, F., Li, P., Huang, B., Gao, F., Ding, C., Wang, C.: Modeling and simulation of grid-connected hybrid photovoltaic/battery distributed generation system. In: China International Conference on Electricity Distribution (CICED), Nanjing, China, pp. 1–10 (2010)
6. Naderi, P., Fallahi, F.: A novel structure proposal for distributed generation using SMES and PV system with relative controllers design. Energy Syst. **6**(2), 153–172 (2015)
7. Alhaider, M., Fan, L.: Mixed integer programming based battery sizing. Energy Syst. **5**(4), 787–805 (2014)

8. De Santis, E., Rizzi, A., Sadeghiany, A., Mascioli, F.M.F.: Genetic optimization of a fuzzy control system for energy flow management in micro-grids. In: IFSA World Congress and NAFIPS Annual Meeting (IFSA/NAFIPS), Edmonton, AB, pp. 418–423 (2013)
9. Natsheh, E.M., Natsheh, A., Albarbar, A.: Intelligent controller for managing power flow within stand-alone hybrid power systems. IET Sci. Meas. Technol. **7**(4), 191–200 (2013)
10. Liao, Z., Ruan, X.: A novel power management control strategy for stand-alone photovoltaic power system. In: 6th International Power Electronics and Motion Control Conference (IPEMC '09), Wuhan, China, pp. 445–449 (2009)
11. Xiong, X., Tse, C., Ruan, X.: Bifurcation analysis of standalone photovoltaic-battery hybrid power system. IEEE Trans. Circuits Syst. I Regul. Pap. **60**(5), 1354–1365 (2013)
12. Elsayed, A.T., Youssef, T.A., Mohamed, A., Mohammed, O.A.: Design, control and management of P-V system for residential applications with weak grid connection. In: 11th Latin American and Caribbean Conference for Engineering and Technology, Cancun, Mexico, pp. 1–10 (2013)
13. Abbes, D., Martinez, A., Champenois, G.: Eco-design optimisation of an autonomous hybrid wind-photovoltaic system with battery storage. IET Renew. Power Gener. **6**(5), 358–371 (2012)
14. Capizzi, G., Bonanno, F., Tina, G.M.: Experiences on the design of stand alone photovoltaic system by deterministic and probabilistic methods. In: International Conference on Clean Electrical Power (ICCEP), Ischia, Naples, pp. 328–335 (2011)
15. Cheng, P., Cheng, C., Hong, S.: Optimal battery chargers for photovoltaic system based on fuzzy theory and Taguchi method. In: International Conference on Advanced Robotics and Intelligent Systems, Tainan, Taiwan, pp. 70–75 (2013)
16. Park, S.M., Park, S.: Power weakening control of the photovoltaic-battery system for seamless energy transfer in micro grids. In: 28rd Annual IEEE Applied Power Electronics Conference and Exposition, Long Beach, CA (2013)
17. Khiareddine, A., Salah, C., Mimouni, M.F.: Power management of a photovoltaic/battery pumping system in agricultural experiment station. Sol. Energy **112**, 319–338 (2015)
18. Salah, C., Lamamra, K., Fatnassi, A.: New optimally technical sizing procedure of domestic photovoltaic panel/battery system. J. Renew. Sustain. Energy **7**(013134), 1–14 (2015)
19. Tofighi, A., Kalantar, M.: Power management of PV/battery hybrid power source via passivity-based control. Renew. Energy **36**, 2440–2450 (2011)
20. Chiang, S.J., Shieh, H.J., Chen, M.C.: Modeling and control of a PV charger system with SEPIC converter. IEEE Trans. Ind. Electron. **56**(11), 4344–4353 (2009)
21. Mohamed, N.S.S., Omar, A.M., Faranadia, A.H.: Assessment of AC coupling PV hybrid system Malaysia. In: IEEE 5th Control and System Graduate Research Colloquium, UiTM, Shah Alam, Malaysia (2014)
22. Papanikolaou, N., Christodoulou, C., Loupis, M.: Introducing an improved bidirectional charger concept for modern residential standalone PV systems. Energy Syst. **6**(1), 21–41 (2015)
23. Majumdar, S., Sapalok, A., Chakraborty, N.: Modeling components of a DC coupled photovoltaic system with maximum power point tracking. In: IEEE 5th Power India Conference, Murthal, India (2012)
24. Almonacid, F., Rus, C., Pérez-Higueras, P., Hontoria, L.: Calculation of the energy provided by a PV generator. Comparative study: conventional methods vs. artificial neural networks. J Energy **36**, 375–384 (2011)
25. Aparicio, M.P., Sebastiá, J.P., Sogorb, T., Llario, V.: Modeling of photovoltaic cell using free software application for training and design circuit in photovoltaic solar energy. In: InTech—New Developments in Renewable Energy, pp. 121–139 (2013). doi:10.5772/51925
26. Rydh, C.J., Sanden, B.A.: Energy analysis of batteries in photovoltaic systems. Part I: Performance and energy requirements. Energy Convers. Manag. **46**, 1957–1979 (2005)
27. Serrao, L., Chehab, Z., Guezennec, Y., Rizzoni, G.: An aging model of Ni-MH batteries for hybrid electric vehicles. In: IEEE Conference on Vehicle Power and Propulsion, Georgia, USA, pp. 78–85 (2005)
28. Achaibou, N., Haddadi, M., Malek, A.: Modeling of lead acid batteries in PV systems. J. Energy Procedia **18**, 538–544 (2012)
29. Abd El-Aal, A.M., Schimd, J., Bard, J., Caselitz, P.: Modeling and optimizing the size of the power conditioning unit for photovoltaic systems. J. Sol. Energy Eng. **128**(1), 40–44 (2006)

30. Frank, S., Rebennack, S.: Optimal design of mixed AC–DC distribution systems for commercial buildings: a nonconvex generalized benders decomposition approach. Eur. J. Oper. Res. **242**(3), 710–729 (2015)
31. Sun, K., Zhang, L., Xing, Y., Guerrero, J.M.: A distributed control strategy based on DC bus signaling for modular photovoltaic generation systems with battery energy storage. IEEE Trans. Power Electron. **26**(10), 3032–3045 (2011)
32. Braam, F., Hollinger, R., Lübeck, C., Müller, S., Wille-Haussmann, B.: Grid-oriented operation of photovoltaic-battery systems. Internationaler ETG-Kongress, Berlin (2013)